

Self-diffusion of adatoms, dimers, and vacancies on Cu(100)

Ghyslain Boisvert* and Laurent J. Lewis†

Département de Physique et Groupe de Recherche en Physique et Technologie des Couches Minces (GCM), Université de Montréal, Case Postale 6128, Succursale Centre-Ville, Montréal, Québec, Canada H3C 3J7

(August 8, 2018)

Submitted to Physical Review B

We use *ab initio* static relaxation methods and semi-empirical molecular-dynamics simulations to investigate the energetics and dynamics of the diffusion of adatoms, dimers, and vacancies on Cu(100). It is found that the dynamical energy barriers for diffusion are well approximated by the static, 0 K barriers and that prefactors do not depend sensitively on the species undergoing diffusion. The *ab initio* barriers are observed to be *significantly* lower when calculated within the generalized-gradient approximation (GGA) rather than in the local-density approximation (LDA). Our calculations predict that surface diffusion should proceed primarily *via* the diffusion of vacancies. Adatoms are found to migrate most easily *via* a jump mechanism. This is the case, also, of dimers, even though the corresponding barrier is slightly larger than it is for adatoms. We observe, further, that dimers diffuse more readily than they can dissociate. Our results are discussed in the context of recent submonolayer growth experiments of Cu(100).

PACS numbers: 68.35.Fx, 71.15.Nc, 71.15.Mb, 68.35.Md

I. INTRODUCTION

Over the years, thin-film growth techniques have become pivotal in the development of new materials and devices. In spite of this, it remains extremely difficult, even impossible, to predict the morphology of the films that would result from a particular set of experimental conditions — temperature, pressure, deposition flux, etc. — even for simple homoepitaxial systems. This state of affairs is due in large part to the fact that growth is determined mainly by kinetic, rather than equilibrium, effects. Since the kinetics of surfaces is determined principally by the diffusion of atoms, either isolated (adatoms) or grouped in small clusters (dimers, trimers, etc.), it is of utmost importance to understand in detail the diffusion mechanisms that are involved in a given temperature range and the rate at which they will proceed. The required information is contained in the temperature-dependent diffusion coefficient and this is the quantity we focus on.

By definition, the diffusion coefficient, D , is given by the Einstein relation

$$D = \lim_{t \rightarrow \infty} \frac{\langle R(t)^2 \rangle}{2dt}, \quad (1)$$

where $\langle R(t)^2 \rangle$ is the mean-square displacement of the particle undergoing diffusion and d is the dimensionality of the space in which the process is taking place. The diffusion coefficient is also often expressed in the Arrhenius form

$$D = D_0 \exp\left(\frac{-E_A}{k_B T}\right), \quad (2)$$

where D_0 is a “prefactor”, k_B the Boltzmann constant, T the absolute temperature, and E_A the activation energy or barrier. This form is rigorously valid in the limit $E_A \gg k_B T$.¹

Experimentally, it is possible to measure directly the diffusion constant by following the displacement of adatoms (or small clusters) over time using field-ion microscopy.² However, because of the high imaging field required, this technique is limited to a few materials, namely W, Ir, Ni, Rh, and Pt. Indirect measurements are also possible, whereby the saturation island density is measured using, for instance, scanning-tunneling microscopy (STM) or low-energy electron diffraction (LEED), then related to the diffusion coefficient using rate equations.³ The problem with such an approach lies, precisely, in the relation between island density and diffusion coefficient (the “scaling relation”): While it is clearly defined when only single adatoms are mobile, it has been shown to become very complicated when larger clusters are involved,^{4,5} thus making it extremely difficult to assess their relative contribution.

In this context, it becomes important to augment the experimental measurements with detailed, accurate, calculations of the diffusion constants based on realistic structural models. This is the route that we follow here. More specifically, we use state-of-the-art simulation methods to calculate the diffusion coefficients of Cu adatoms and dimers, as well as vacancies, on the Cu(100) surface. Two distinct computational approaches are used: First, molecular-dynamics (MD) simulations, based on the semi-empirical embedded-atom method (EAM), are carried out; this provides us with

qualitative knowledge of the processes involved during diffusion, as well as quantitative information on the diffusion coefficients for various mechanisms, in particular the prefactors. This is extremely important since only dynamical simulations can provide accurate values for the prefactors, which can vary significantly as a function of the barrier height.⁶ The activation energies, in contrast, can be calculated accurately using static (0 K), energy-minimization methods, as we will demonstrate. In order to go beyond the approximate EAM, we have performed, second, detailed *ab initio* calculations of the energy barriers. Calculations were done within the framework of density-functional theory (DFT),⁷ using both the all-electron (AE), full-potential, linear-muffin-tin-orbital method (FP-LMTO),⁸ and the now-standard pseudopotential-plane-wave (PP-PW) approach.⁹ In the latter case, since it has been shown that the inclusion of gradient corrections to the exchange-correlation energy leads to a significant improvement over the usual local-density approximation (LDA) for *3d* metals,^{10,11} most calculations have been performed in the generalized-gradient approximation (GGA); some LDA results are nevertheless presented in order to compare with a previous study by Lee and coworkers.¹²

The reasons for studying the system Cu/Cu(100) are manifold. First, simplicity: the surface lattice is square and, because the system is homoepitaxial, only one type of chemical species need be considered (i.e., modeled) and no large stress, e.g., arising from mismatch, will be involved. Such simple systems — homoepitaxial face-centered cubic metals — have been the object of numerous studies of the fundamental aspects of growth (see for instance Refs. 5,13–21). Second, surface diffusion on Cu(100) has been studied in detail both experimentally^{22–25} and theoretically.^{12,26–40} (Of the latter, only Ref. 12 is a first-principles calculation.) Yet, no clear picture has emerged: While experiment indicates a barrier in the range 0.28 to 0.40 eV, but gives no information on the actual mechanism *via* which diffusion takes place,^{22–25} the *ab-initio* calculations of Lee *et al.*¹² predict that diffusion proceeds primarily through simple hopping of an adatom on the surface, with a barrier height of 0.69 eV. In comparison, studies based on various semi-empirical potentials give values in the range 0.20–0.70 eV and are in disagreement on the preferred diffusion mechanism.^{26–40}

Evidently, the dominant mechanism for diffusion on Cu(100) is not resolved. The various processes examined here — jump and exchange for the adatom and the dimer, and jump only for the vacancy — are illustrated in Fig. 1. Although there are other possibilities, especially at high temperatures,³² the ones we consider are found, from our MD simulations, to be the best candidates for low-temperature diffusion. We computed, in addition, the diffusion coefficient for an adatom moving along a step in order to understand the shape of islands on (100) terraces.

Our LDA calculations of the energy barrier for adatom

diffusion corroborate the previous study, also within LDA, by Lee *et al.*;¹² however, we find the barrier to be *significantly* reduced when calculated within the GGA, thus bringing it much closer to the experimental value. In any case, the preferred mechanism for diffusion is found to be hopping. We find the barrier for dimer diffusion to be close to that for the adatom, but lower than that for dimer dissociation. We also find that vacancies are more mobile than adatoms and that diffusion of adatoms along a step proceeds much more rapidly than on a terrace so that the island shape during growth should be close to equilibrium. Prefactors, finally, do not depend sensitively on the species undergoing diffusion. These findings are discussed in the context of recent growth experiments performed on this system.^{22–25}

II. COMPUTATIONAL DETAILS

A. Semi-empirical calculations

As mentioned already, the atoms in the MD simulations were assumed to interact *via* the EAM potential proposed by Foiles, Baskes, and Daw;⁴¹ the optimized parameterization of Adams, Foiles, and Wolfer⁴² was used. Although this model has been fitted to bulk properties, it has been applied successfully to the study of various surface phenomena.⁴³

For the MD calculations on the flat (100) surface, we used a geometry and a procedure similar to our previous study of adatom diffusion on Ag and Au surfaces.⁴⁴ The surfaces were approximated by slabs containing 8 layers (excluding the adatom) of which the bottom two are held fixed in order to mimic the bulk. Each of the layers contains 64 atoms. For the diffusion along a step, we considered a (13,1,1) surface, which is vicinal to the (100) surface, and possesses 6-atom wide terraces. In order to keep the rectangular shape of the unit cell, two steps are included at the surface. (In the (100) direction, the planes are stacked in the order *ABAB...*). Each of the two terraces contains 36 atoms and we thus have 72 atoms per layer. The same number of layers as in the case of the (100) surface was used. When studying diffusion, an adatom is added at each of the two steps. In all cases, periodic boundary conditions were applied in the lateral directions, i.e., parallel to the surface, so that the system is effectively infinite in the $x - y$ plane. The lattice parameter of the rigid layers was determined from a series of runs on the bulk material in the (N, P, T) ensemble (using a 256-atom system) at each simulated temperature. All others simulations are carried out in the (N, V, T) ensemble.

In most cases studied here, it is necessary to deal with more than one diffusion mechanism for a given species, viz. jump and exchange. It is simpler, then, to consider the frequency at which each type of event is taking place, rather than the actual rate of diffusion as given by Eq.

1. As we observed in a previous article,⁴⁴ when the barriers are high enough, diffusion can be assimilated to a random walk, so that the diffusion coefficient is simply related to the frequency of events. We will see, in Sec. III C, that the barriers are indeed high compared to the temperature at which diffusion is considered. In order to determine the frequencies, the evolution of the diffusing species (adatom, dimer, or vacancy) is followed at several temperatures (see Sec. III) for a time long enough to yield reliable and reproducible statistics. In practice, the runs consisted of a period of equilibration of 48 ps, followed by a period of “production” of 5–18 ns (depending on the number of events observed, i.e., barrier and prefactor for the process, as well as temperature), during which statistics were accumulated. A timestep of 2.4 fs was used to perform the numerical integration of the equations of motion. To speed up the calculations, we introduced a cutoff distance in the potential, beyond which all interactions were neglected. It was found that a cutoff of 4.8 Å (between third and fourth-neighbor shells) yields barriers within 5% of their converged values except in the case of the dimer, for which a cutoff of 5.4 Å (between fourth and fifth-neighbor shells) was necessary to achieve the same level of accuracy.

In order to determine the 0 K, static barriers and compare them with their dynamical equivalents, we also carried out a series of energy-minimization, “molecular-statics” (MS), calculations, whereby the atoms are moved iteratively in the directions of the forces acting on them until these vanish (“relaxation”). The static energy barrier is obtained by relaxing the system in both the equilibrium and the transition state; in the latter case, a constraint is used to maintain the particle(s) at the saddle point and minimization is carried out with respect to all other degrees of freedom.

B. *Ab initio* calculations

Since first-principles MD for transition metals is too demanding for a direct study of diffusion, only MS calculations of the barriers were carried out using this approach. First, following our study of diffusion on Ag, Au, and Ir,⁴⁵ we computed the energy barriers using the FP-LMTO.⁸ This method is approximate only in the parameterization of the exchange-correlation energy; however, it provides no analytical forces on the ions so that relaxation effects cannot be estimated accurately. To overcome this problem, we also performed, second, calculations using the PP-PW approach, where the ionic-core potential is approximated by a pseudopotential. In this case, fully self-consistent calculations were carried out using both the LDA and the GGA, whereas only the LDA was used in the case of FP-LMTO. We now describe our computational approach in more detail.

For the FP-LMTO calculations, we used the same approach as in Ref. 45. The surface was constructed in supercell geometry, and consisted of a slab of 5 to 9 layers and a vacuum region of about 10 Å periodically replicated in space; each layer contains 4 to 9 atoms. Both the number of layers and the number of atoms per layer were varied in order to ensure convergence with respect to system size (see below). To determine the barriers for diffusion, an adatom was placed on each of the two external surfaces of the slab, with the central layer taken as a mirror plane in order to reduce the computational load. Only adatom jump diffusion was considered using this technique. The z coordinate of the adatom was varied in order to minimize the total energy of the slab. All other atoms were kept in their ideal, bulk-like position, except for the surface layer, which was relaxed before the adatom was introduced (i.e., in its clean state) using a 5-layer (1×1) unit cell.

To compute the energy, we used a basis set of 27 functions per atom, consisting of $4s$, $4p$, and $3d$ functions with kinetic energy $-\kappa^2 = -0.7, -1.0, \text{ and } -2.3$ Ry, respectively. Scalar-relativistic corrections were included and the exchange-correlation energy evaluated using the Ceperley-Alder form.⁴⁶ The integration over the Brillouin zone employed 36 equidistant \mathbf{k} points when using 4 atoms per layer, and 16 when using 9 atoms per layer; a Gaussian broadening of 20 mRy was used to ensure the numerical stability of the integral. Bulk and clean surface properties were calculated using the same density of \mathbf{k} points.

2. PP-PW

In the PP-PW approach, the core orbitals are replaced by pseudopotentials. Here, we used pseudopotentials generated according to the semi-relativistic scheme of Troullier and Martins,⁴⁷ and cast in the fully-separable, norm-conserving form of Kleinman and Bylander, with the s component only being local.^{48–50} The $3d$ electrons were treated as valence states. The electronic wavefunctions were expanded in plane waves with a kinetic energy cutoff of 60 Ry in the LDA⁴⁶ and 65 Ry in the GGA.⁵¹ The \mathbf{k} -space integration was performed using a set of 9 equidistant points in the surface Brillouin zone for the systems with 4 atoms per layer and 4 points for the ones with 9 atoms per layer. To improve convergence, the electronic states were occupied according to a Fermi distribution with a temperature of $k_B T_{el} = 0.1$ eV and the total energy extrapolated to zero electronic temperature. For similar reasons, the *initial* wave-functions were obtained from the self-consistent solutions of the Kohn-Sham Hamiltonian in a mixed-basis set composed of pseudo-atomic orbitals and plane waves with kinetic energy less than 4 Ry.⁵² The minimization of the energy

with respect to the electronic degrees of freedom was done iteratively using a Car-Parrinello-like technique.^{53,54}

In view of the high energy cutoff needed in the plane-wave expansion, it is important to keep the system size to a minimum. To do so, we used a geometry slightly different from that described above, considering here a single adatom on one surface of the slab. This enables us to use a smaller number of layers and, therefore, a smaller supercell. In practice, 3 to 7 layers were considered, with only the adatom and at most the top two layers allowed to relax. Damped Newton dynamics was used to displace the atoms; this was done iteratively until all forces (on the atoms allowed to relax) became less than 0.01 eV/Å. Bulk and clean surface properties were calculated using the same \mathbf{k} -point density as in the diffusion study; for the clean surface, a 9-layer, (1×1) cell was used.

3. Bulk and clean (100) surface

In order to establish the validity of our *ab initio* approach, we have computed, prior to considering diffusion, the bulk lattice constant and some properties of the clean (100) surface, namely the surface energy, surface relaxation, and work function. The results are listed in Table I along with other *ab initio* results and available experimental data.

For the lattice constant, first, we get good overall agreement with previous calculations. It is well known that the LDA underestimates lattice constants. The GGA, however, tends to overcompensate and, as a result, the GGA lattice constants are usually larger than experiment,¹⁰ as indeed found here. Also, as noted by Lu and coworkers,⁵⁷ pseudopotential calculations yield lattice constants larger than all-electron (AE) calculations, also a feature observed here. The combination AE-GGA, therefore, seems to be optimal (but not available to us at present); this is also supported by the fact that the GGA provides a much better description of the cohesive energy than the LDA.¹¹ Thus, even though the PP-PW-GGA combination does not yield accurate lattice constants, it is better suited to describing Cu than PP-PW-LDA.

For the clean (100) surface, now, our results are also in relatively good agreement with other calculations, when available, and with experiment. It is interesting to note that, even if AE and PP calculations give different values for the lattice constant, they lead to very similar surface properties for a given level of approximation of the exchange-correlation energy (i.e., LDA or GGA). Thus, a self-consistent PP calculation is quite suitable to describe surface properties here, even if bulk properties are not as well described as in AE calculations. We note from Table I that the GGA reduces the surface energy and the work function compare to the LDA. This effect of the GGA on metallic surfaces has already been predicted from jellium calculations.⁵¹ The same phenomenon has been observed on Cu(111),⁶⁹ Pt(111),⁷⁰ and Ag(100).⁷¹ In view of the

difficulty in measuring accurate surface energies, and the scatter in the experimental values for the work function, it is not clear which exchange-correlation functional best describes surfaces properties. However, considering that the GGA provides a better description of bulk Cu, we conclude that it is better suitable, also, for Cu surfaces.

III. RESULTS

As we previously have shown,⁴⁴ adatom diffusion barriers can be reliably extracted from static calculations. However, in order to determine completely the diffusion coefficient, the prefactor is also needed, and there seems to be no simple way of extracting this quantity with sufficient accuracy from purely static calculations. On the other hand, first-principles MD simulations are too demanding in terms of computer time for such an enterprise to be undertaken, and one must therefore resort to classical models in order to calculate the prefactors. We present here the results of our study of diffusion on Cu(100) using both a classical and a quantum description of forces for calculating the energy barriers, and classical MD for estimating the prefactors.

It is often assumed, for convenience and without much justification, that prefactors for diffusion are constant (see, e.g., Ref. 2), independent on the details of the surface. However, in a recent study,⁶ we have shown that the diffusion of adatoms follows the compensation (Meyer-Neldel) law and, as a result, prefactors can vary by several orders of magnitude. The Meyer-Neldel rule states that, for a family of Arrhenius processes,

$$X = X_0 \exp(-E_A/k_B T) \quad (3)$$

(which is the case of diffusion, Eq. 2), the prefactor X_0 depends exponentially on the activation energy E_A :

$$X_0 = X_{00} \exp(E_A/\Delta_0), \quad (4)$$

where Δ_0 is the iso-kinetic (or Meyer-Neldel) energy and X_{00} is a constant. It is therefore important, in order to determine the most mobile species in a given temperature regime, to see how prefactors compare. These results will be presented in Sec. III C. We discuss, first, the static energy barriers, both in the context of EAM and from first principles.

A. Static energy barriers – EAM

1. Adatoms

Our results for the static barriers on Cu(100), $E_{A,i}^0$, for the various cases of diffusion considered here, are listed in Table II; our results generally agree with previous estimates using a similar theoretical framework.^{26,33,36,39}

The adatom, within the EAM picture, is found to diffuse preferably *via* a jump mechanism, the barrier for exchanges being much higher — 0.73 vs 0.50 eV. From these values of the barriers, one would conclude that exchange diffusion contributes negligibly to mass transport (in comparison to jump diffusion). However, as we will see in Sec. III C, this conclusion must be taken with caution because the prefactor for exchanges is much larger than that for jumps.

2. Dimers

In order to determine if small clusters are mobile at low temperatures, or if, rather, they are more likely to dissociate, we have calculated the barriers for the jump and exchange diffusion of dimers, as well as the binding energy, dissociation energy, and excess energy of metastable vs equilibrium state. The results are listed in Tables II and III.

Just like adatoms, dimers diffuse much more easily by jumps than by exchanges, and the barriers for the two processes are very similar to the corresponding ones for adatoms. Thus, as far as the mechanism is concerned, adatoms and dimers behave in the same way; if we consider only the barriers, dimers are expected to be mobile at the same temperature as the adatoms.

It is important to note that, for dimers, the barrier for jump diffusion (0.49 eV — cf. Table II), is the barrier to go from the equilibrium to the metastable state, as depicted in Fig. 1(c). Indeed, the barrier to go from the metastable to the equilibrium state, which is equal to the barrier height minus the excess energy of the metastable state ($0.49 - 0.29 = 0.20$ eV — cf. Table III), is much smaller than the reverse; the corresponding process thus occurs much faster. The limiting process, therefore, is the one considered here, i.e., equilibrium to metastable.

The dissociation barrier for a dimer is given, approximately, by the sum of the diffusion barrier for the adatom and the binding energy of the dimer.⁵ In the present case, this leads to a barrier of 0.85 eV. Direct calculation of the dissociation barrier is difficult considering that there are several possible dissociation pathways. We have examined different possibilities and found the lowest barrier to be 0.81 eV (corresponding to a 50% stretch of the dimer along its equilibrium axis), in good agreement with the approximate value above, and significantly larger than the barriers for diffusion. Thus, dimers are already mobile at temperatures well below the onset of dissociation.

We now compare mass transport from dimers and adatoms, considering only the predominant jump-diffusion process. To do so, it is necessary to first determine the mean-square displacement of the center of mass of the dimer during an event. When a dimer jumps, there exists 4 different paths leading to a zero net displacement of the center of mass, 4 leading to a displacement of $a^2/2$, and 8 leading to a displacement of $a^2/4$, where a is the

lattice constant. On average, therefore, the mean-square displacement is $a^2/4$. This is a factor of 2 smaller than the corresponding displacement for an adatom, but the dimer contains 2 atoms; hence, as much mass is transported in a single event as is in the case of adatoms, on average. We are thus led to conclude that, within EAM, *dimers contribute as much to mass transport as adatoms.*

3. Vacancies

While vacancy diffusion is not, *per se*, a mechanism for growth, it can have important consequences on mass transport, in particular in the process of annealing defected surfaces. In Fig. 1, we show the mechanism by which a vacancy diffuses on the (100) surface — basically a jump. The corresponding barrier is 0.47 eV (cf. Table II), larger than the value of 0.35 eV reported in Ref. 36, which is in error.⁷²

The jump-diffusion barrier for vacancies is, also, close to that for adatoms. Of course, the actual contribution of each process depends on the relative population of the two species, which itself depends on the formation energies; indeed, the migration energy is the sum of the formation energy and the diffusion barrier. Using EAM, Karimi and coworkers³⁶ found formation energies of 0.59 and 0.71 eV for the vacancy and the adatom, respectively. Thus, vacancies have lower formation energy than adatoms and should therefore contribute more to mass transport. However, during growth, a large reservoir of adatoms is available, and their mobility is limited only by the diffusion barrier. In contrast, vacancies first have to form, i.e., their mobility is determined by the diffusion barrier *plus* the formation energy, and thus severely reduced, to the point where their contribution to mass transport will in fact be negligible at temperatures of interest.

4. Steps

The shape of islands on otherwise flat terraces is important for a proper understanding of growth phenomena. It is determined, in equilibrium conditions, by the energies of the various steps defining its perimeter. During growth, the equilibrium shape can be attained only if the kinetic processes leading to equilibrium are fast enough to overcome the continuous arrival of new adatoms onto the island. For the (100) surface, the equilibrium island shape is approximately square, with the corners rounded. The sides of the island are formed by $\langle 110 \rangle$ -oriented steps, which are the most densely packed on this surface. Thus, if diffusion along these steps, which measures the rate at which equilibrium is reached, is fast compared to diffusion on a terrace, corresponding to the rate at which adatoms arrive, then the shape will be close to equilibrium. We find, for diffusion along $\langle 110 \rangle$ steps, a barrier

value of 0.26 eV (cf. Table II); this is indeed much lower than the barrier for adatom diffusion on terraces, 0.50 eV. Thus, the shape of islands is expected to be close to equilibrium *even* during growth.

B. Static energy barriers – *Ab initio*

1. Adatoms

In order to assess the validity of the EAM calculations, we move on with a discussion of *ab-initio* diffusion barriers, starting with the case of adatoms which, in view of the discrepancy between the first-principles calculations of Lee *et al.*¹² and experiment, constituted the initial motivation of this work. Also we have, for adatoms, carried out an extensive study of convergence with respect to size and other parameters of the model; the results are presented in Table IV.

A first observation from Table IV is that, within numerical accuracy, the AE-FP-LMTO and PP-PW calculations give the same result for the jump-diffusion barrier for cells of equivalent size, at the same level of approximation (compare, e.g., the FP-LMTO-LDA and PP-PW-LDA for jumps on the (2×2) cell with 5 or 7 layers). Thus, the use of PP’s seem to have little effect on diffusion barriers even if it yields lattice constants different from AE calculations. The same behavior was observed for clean surface properties, as mentioned in Sec. II B 3. This establishes the validity of the approach and only PP calculations will therefore be discussed from now on.

Within the PP-PW scheme, forces on the ions are easy to compute and the effect of relaxation on diffusion barriers can be assessed. This question was neglected in our previous study of self-diffusion on Ag, Au, and Ir surfaces using the FP-LMTO technique, for which analytical forces are not available in the supercell geometry.⁴⁵ From the PP-PW-LDA results for the 3-layer, (2×2) cell given in Table IV, it is clear that the effect of relaxation on the barrier for jumps is negligible (0.75 eV for the unrelaxed surface, indicated by the superscript “*u*”, vs 0.74 eV for the relaxed surface). Evidently, this is more important for the exchange process, but nevertheless small (1.23 vs 1.18 eV, i.e., less than 5%) — smaller in fact than could be expected.

In most calculations, only the top layer of the slab was allowed to relax (in addition to the adatom). We have verified that this is not a limiting approximation by carrying out some calculations where, also, the second layer was relaxed. This is indicated by the superscript “2” in Table IV for the 4-layer, (2×2) cell under PP-PW-LDA. The effect is extremely small, no more than 0.01 eV, i.e, within the accuracy of the method. One must not generalize these conclusions to other systems, however, especially the (111) surface of fcc metals where barriers for jumps are small. For instance, for Cu diffusion on Cu(111), the barrier drops by a factor of almost two, from

0.14 to 0.08 eV, when allowing the first atomic layer to relax;⁶⁹ similar effects are also found for Pt/Pt(111).⁷⁰

The convergence with respect to supercell size was examined very carefully. As can be seen from the PP-PW-LDA results in Table IV, the barriers for both processes “oscillate” slightly when increasing the number of layers beyond 4. In the case of exchanges, the fluctuations in the barrier height are more important than for jumps in absolute value, but quite similar on a relative scale, viz. about 10%. We note also that the barrier for jumps does not change noticeably upon increasing the lateral size of a 3-layer slab from (2×2) to (3×3) , while the barrier for exchanges drops by about 11%.

Since the barrier for jumps remains the same upon going from a (2×2) to a (3×3) cell, we conclude that our error on this energy is essentially that arising from the convergence with respect to the number of layers, i.e., about 10%. For exchanges, we observe the barrier to vary a bit upon going from a (2×2) to a (3×3) cell, but we expect that it should not change substantially for larger systems. Thus, the error on the barrier for exchanges is expected to be about the same as for jumps, namely about 10%.

Finally, we also verified the convergence of the results with respect to Brillouin-zone sampling, again for the 4-layer, (2×2) cell under PP-PW-LDA. We found, upon increasing the number of (surface) \mathbf{k} -points from 16 to 25, the barriers for jumps and exchanges to change very little — by 0.02 and 0.03 eV, respectively, considering only relaxation of the top substrate layer.

As mentioned earlier, we know of only one other *ab-initio* calculation of the barriers for adatom diffusion on Cu(100), by Lee and coworkers,¹² carried out within the LDA. Using a 3-layer (3×3) cell, they found activation energies of 0.69 eV for jumps and 0.97 eV for exchanges. This compares quite well with our results for the same cell size, as can be seen in Table IV. The small differences are likely due to different Brillouin-zone sampling schemes: while we used a 2×2 grid of equidistant points for this cell, Lee *et al.* employed only the Γ point.

The GGA, as we have seen above, yields a better description of bulk Cu properties, such as lattice constant and cohesive energy, compared to the LDA.^{10,11} We have also found in Sec. II B 3 that it has an effect on surface properties such as the surface energy and the work function. It is therefore of interest to see how diffusion barriers compare in the two approximations. This question was addressed recently in the case of Ag/Ag(100) by Yu and Scheffler;⁷¹ for Ag, the GGA is known to overcompensate the LDA error as far as the lattice constant is concerned.¹⁰ Yu and Scheffler found, under the GGA, the barriers to drop from 0.52 to 0.45 eV in the case of jumps, and from 0.93 to 0.73 eV for exchanges, a decrease of respectively 13% and 22% from the LDA value. In a recent experiment, Langelaar *et al.*⁷³ found a diffusion barrier of 0.43 ± 0.02 eV, assuming a prefactor of 10 THz as obtained from MD simulations.⁴⁴ This agrees within error with the above GGA value for jumps; however, the

LDA value is not far either and it is therefore difficult to say which approximation is better. In the present case, the GGA barriers are about 22% smaller than the corresponding LDA values (cf. Table IV). This is larger than the numerical accuracy estimated earlier — about 10%. We are therefore led to conclude that the GGA leads to a significant decrease of energy barriers compared to the LDA.

Our best estimates for the activation energies are thus 0.52 ± 0.05 and 0.96 ± 0.10 eV, for jumps and exchanges, respectively. Thus, just as was the case with EAM, the adatom is found to diffuse more readily *via* a jump mechanism. In fact, as can be seen from Table II, the EAM barrier for jumps is in quantitative agreement with the GGA barrier. We thus expect MD/EAM simulations to yield a reliable, *quantitative* estimate of the prefactor for jump diffusion (see below). For exchanges, the EAM underestimates the barrier with respect to the GGA and, therefore, the MD simulations can only yield qualitative information.

2. Dimers

For dimers, now, we have not performed detailed convergence tests, but error bars can be estimated from the above convergence study for adatoms: Since the coverage for a dimer on a (3×3) cell is comparable to that for a single adatom on a (2×2) cell, the error on the barriers for exchange diffusion should be approximately the same, namely 20%, while other quantities — barriers for jumps, binding energies, and excess energies of the metastable configuration — should be accurate to about 10%. All the results discussed below refer to a 4-layer, (3×3) unit cell.

Dimers are found to diffuse preferentially *via* jumps, as was the case also for adatoms, with a barrier of 0.57 eV compared to 0.79 eV for exchanges (cf. Table II). The barrier for jumps estimated from EAM compares well with the GGA value, as was also true of adatoms, although the deviation here is a bit larger. For exchanges, the EAM and PP-PW-GGA estimates are in good agreement, but in view of the large error bar on the latter, it is difficult to ascertain that this agreement is genuine.

As already noted in Sec. III A 2, the barrier towards dissociation is given, roughly, by the sum of the dimer binding energy and the diffusion barrier of the adatom.⁵ No attempt to compute this quantity directly from first principles has ever been made because of the prohibitively large system size required. Using the approximate form, we obtain a dissociation barrier of 0.74 eV (cf. Table III), much higher than the barrier for diffusion. Thus, we conclude that dimers are mobile at temperatures lower than those for which dissociation takes place. This is in qualitative agreement with EAM, even though quantitatively, the difference between barriers for diffusion and for dissociation is larger within EAM than

within GGA, due to the combined effect in EAM of a lower diffusion barrier and a higher dissociation barrier. The difference in the dissociation barrier can be traced back to the dimer binding energy, which is much lower within GGA than within EAM.

In view of the large excess energy of the metastable configuration with respect to equilibrium, 0.35 eV, which agrees well with EAM, the discussion on mass transport presented in Sec. III A 2 remains valid: the relative contributions to mass transport by adatoms and dimers can be determined solely on the basis of their jump frequencies. Since the energy barrier for dimer diffusion is slightly larger than that for adatoms — 0.57 vs 0.52 eV — we conclude that adatoms will be mobile at lower temperatures than the dimers. In view of the small difference, however, the temperature range in which the above conclusion is valid will be rather narrow.

3. Vacancies

The barrier for the diffusion of vacancies was also determined *ab initio* using the GGA. Its value, given in Table II along with other barriers, is estimated to be 0.42 eV, with an error bar of at most 20%. Again, the agreement with the EAM result, 0.47 eV, is striking. Also, this is smaller than the barrier for adatom jump diffusion. Thus, vacancy diffusion should dominate mass transport on the surface except, as discussed in Sec. III A 3, during growth, when a large “reservoir” of adatoms is available.

As can be concluded from Table II, the present EAM parameterization provides, in most cases, a very satisfactory agreement with the first-principles results we have just described, taking due account of the uncertainties of the *ab initio* calculations. This is a bit of a particular case, however: we have shown, in a recent publication,⁴⁵ that the agreement between EAM and first-principles calculations could be quite acceptable when the barriers are large, but poor when they are small, as is the case for instance on the (111) surface of fcc metals.

C. MD-EAM

1. Adatoms

While static calculations of diffusion barriers on Cu(100) have been numerous, direct simulations of the actual diffusion processes have been rather scarce.^{17,32,37,38,74} Of these, only Ref. 38 is concerned with a detailed Arrhenius study of adatom diffusion, and dimer and vacancy diffusion was not considered. Also, the model used, based on a tight-binding description of the interatomic potentials, differs from ours. For consistency, and in view of the fact that the barriers for diffusion of adatoms, dimers, and vacancies are comparable,

as we have just seen, we provide here a detailed discussion of our MD/EAM simulations, with particular emphasis on prefactors which are not available from static approaches, starting with the case of adatoms. (See also Sec. 5, below.)

MD simulations were performed at several temperatures between 650 and 900 K. The lower end of the range corresponds to the limit for accumulating proper statistics, while the upper end corresponds to the onset of surface disordering, i.e., spontaneous creation of adatom-vacancy pairs. At high temperatures, “exotic” mechanisms, such as long exchanges involving several atoms, are present but to a much lesser extent than the usual jump and exchange mechanisms. In view of the much higher energy barriers associated with these exotic processes, and the exponential behavior of the diffusion coefficient (see Eq. 2), their contribution to mass transport at low temperature will be negligible. These will therefore be ignored here, since we are primarily interested in low-temperature growth.

In Fig. 2, we present Arrhenius plots of the frequency of jump and exchange events for the adatom. The corresponding parameters — attempt-to-diffuse frequencies (prefactors) Γ_0 and energy barriers E_A — are listed in Table II. We find that the barrier for jump diffusion is significantly smaller than that for exchanges, as was found also in the MS calculations. In contrast, not available from MS, the prefactor for exchange is found to be *much larger* — by a factor of about 20 — than that for jumps, in qualitative agreement with the compensation law, eq. 4. This is an important result: Because the barrier for exchanges is so much larger than that for jumps, the former would hardly be observable on the MD timescale if it was not of compensation. In fact, from Fig. 2, we see, as another consequence of compensation, that diffusion crosses over from a regime where jumps predominate at temperatures lower than ~ 750 K to a regime where exchanges take over. If one thinks in terms of mass transport, rather than frequencies, the crossover temperature is even lower, ~ 650 K, because the mean-square displacement associated with an exchange event is twice as large as that for a jump (cf. Fig. 1). At low temperatures, evidently, compensation is not strong enough to overcome the difference in barriers. For example, at 300 K, using the present Arrhenius parameters, we would observe, on average, 150 jumps for a single exchange event.

2. Dimers

The barriers for dimer diffusion, we have found in the MS calculations, are very similar to the corresponding ones for the adatom within EAM. It is thus of interest to examine how prefactors compare in order to determine the dominant contribution to mass transport.

An Arrhenius plot of the frequency of jumps and exchanges is given in Fig. 3; the corresponding parameters

are listed in Table II. Again, here, exotic diffusion mechanisms can take place at high temperatures (e.g., jumps involving the concerted motion of the atoms forming the dimer), but they are present to a lesser extent than the two mechanisms depicted in Fig. 1 and can be neglected in the study of low-temperature growth. The jump is the preferred mechanism for diffusion at low temperatures, with a barrier about 0.25 eV smaller than that for exchanges. The prefactors, however, show the opposite behavior, i.e., compensation again is present. In this case, the crossover occurs at about 900 K, somewhat higher than for adatoms.

It is quite remarkable that the jump and exchange diffusion barriers are the same, within error, for adatoms and dimers. Likewise, the prefactors are essentially equivalent: the observed differences, $\sim 50\%$, are hardly significant in that they could easily be absorbed in variations of the exponential factor that could arise from small errors in the energy barriers. Thus, for all practical purposes, the two species behave in a similar manner, as can in fact be seen in Fig. 3, and thus contribute equally to mass transport within EAM.

3. Vacancies

Fig. 4 shows the Arrhenius frequency of jumps for the vacancy; the corresponding parameters are listed in Table II. No other processes provide a significant contribution to diffusion though we have observed, at high temperatures, some rare long-jump events. Clearly, the vacancy and the adatom display similar behavior, with perhaps a slight edge to the vacancy, both in terms of energy barriers (0.47 vs 0.49 eV) and prefactors (27 vs 20 THz); the GGA predicts an even lower barrier for vacancies. Thus, as far as mass transport is concerned, the two processes contribute in essentially the same way during a single event.

4. Steps

Finally, in Fig. 5, we display the frequency of jumps for diffusion along a $\langle 110 \rangle$ step on the (100) surface. The frequency of jumps on the clean surface is also shown for comparison. The Arrhenius parameters are given in Table II. The barrier for diffusion along the step is twice as small as that for jumps on an infinite, flat (100) surface as was predicted from MS calculations. In spite of the fact that the prefactor is roughly one order of magnitude smaller than on the terrace (3 vs 20 THz), diffusion along the step is much faster due to its relatively low barrier. For instance, at 300 K, diffusion along a step is ~ 2000 times faster than on a terrace. Thus, it is certainly the case that an island, upon the arrival of an adatom from the terrace, has time to rearrange itself into its equilibrium shape before another adatom comes in. In other

words, islands remain close to equilibrium during growth.

5. Final Remarks

Before moving on to a discussion of our findings in the context of growth experiments, a few remarks are in order. First, we find, in all cases examined, the static activation energy to lie very close to the corresponding barrier determined from detailed, extensive MD simulations, as can be seen from Table II. This indicates that, at least for the system under consideration here, *accurate* energy barriers can be obtained from purely static, first-principles calculations. This is at variance with the results of Tully and coworkers,⁷⁵ who found, using a “ghost-particle approach” and a Lennard-Jones potential, the dynamical barrier for the dimer to differ from the static one. Likewise, Evangelakis and Papanicolaou,³⁸ using a tight-binding description of the interatomic potentials, found a dynamical barrier lower than the static one for adatom exchanges on Cu(100). In the latter case, however, the statistics are much poorer than ours; we found, in fact, that their diffusion data, within the statistical uncertainties, can readily be accommodated by an Arrhenius law with a barrier equal to the static value. Second, we find that, given an energy barrier, the attempt-to-diffuse frequencies (prefactors) are similar, regardless of the species undergoing diffusion. Third, although it is difficult to draw firm conclusions from the data presented above, it seems that, not surprisingly, the compensation law is valid not only for adatoms,⁶ but also for dimers and vacancies. Based on our second remark above, it would appear that the *same* set of Meyer-Neldel parameters — X_{00} and Δ_0 (cf. Eq. 4 — could describe diffusion frequencies for the adatom, the dimer, and the vacancy; more calculations are however required to assess this point in more detail.

IV. DISCUSSION

To our knowledge, there exists four different experimental determinations of the diffusion barrier of a Cu adatom on Cu(100).^{22–25} As mentioned in the Introduction, the values reported in these vary quite a bit, from 0.28 to 0.40 eV, and do not agree with those calculated so far; diffusion on this surface, evidently, is not well understood. We discuss here the results of our calculations in the light of these experiments.

In the first experiment,²² the diffusion barrier was inferred from a study of growth via step propagation. The diffusion coefficient, indeed, can be related to the mean size of terraces; by measuring this quantity as a function of temperature, between 318 and 415 K, and fitting to an Arrhenius law, a barrier of 0.40 eV and a diffusion prefactor of 1.4×10^{-4} cm²/s, were obtained. The energy barrier is quite a bit smaller than the one we obtained for

adatom or dimer jumps, which dominate diffusion as we have seen earlier, about 0.50 eV. The experimental prefactor corresponds to an attempt-to-diffuse frequency of 0.8 THz, more than an order of magnitude smaller than the EAM result. In view of the good agreement between EAM and *ab initio* calculations for the barriers for jumps, we expect the calculated attempt-to-diffuse prefactors to be correct within at most an order of magnitude, thus in disagreement with the experimental value. In fact, if we extrapolate the calculated diffusion coefficient to temperatures in the range 318–415 K, we find agreement within a factor of two with experiment, thus suggesting that indeed there is a possibility that both the prefactor and the barrier in Ref. 22 are underestimated. One possible explanation for the disagreement is that species other than adatoms, such as dimers, might be present experimentally, in view of the relatively high temperature, and contribute to diffusion.

Using low-energy ion scattering (LEIS), second, Bree-man and Boerma²³ obtained a diffusion barrier of 0.39 ± 0.06 eV, *assuming* a prefactor of 10 THz — quite a bit larger than the value of 0.8 THz estimated from step propagation measurements (see above). In these experiments, adatoms are created by the ion-beam irradiation of a surface. Their concentration can be estimated from the LEIS yield, which changes as a function of temperature because of diffusion towards — and incorporation into — the steps between terraces (sometimes referred to as “annealing”). An abrupt change in the LEIS yield signals the onset of adatom mobility; given the timescale of the experiment and the length of the terraces, it is then possible to determine the diffusion coefficient. Assuming a value for the the prefactor, finally the diffusion barrier can be extracted. It should be stressed that these measurements are carried out at a single temperature; this is the reason the prefactor must be assumed in order to determine the activation energy, leading to possibly large errors.

In addition to adatoms, however, surface vacancies can also be created during irradiation. It is not clear what their effect is on annealing. Our calculations indicate that they have a diffusion barrier lower than adatoms. Thus they could, for example, recombine with neighboring, immobile, adatoms. Experiment, therefore, would measure the onset of mobility of vacancies rather than adatoms. This question has been discussed in Ref. 76, where it is argued, on the basis of an empirical model, that vacancies start diffusing at about 120 K and are all annealed (into steps) by the time temperature reaches the adatom mobility edge, about 140 K; i.e., vacancies would *not* affect diffusion. However, our *ab-initio* barrier for vacancy diffusion is in good agreement with the activation energy determined from LEIS — 0.42 vs 0.39 eV — and we must therefore conclude that the diffusion of vacancies remains a possible explanation for the observed onset of mobility. We note that in the case of Ag/Ag(100)⁷³ (see also Sec. III B 1), also using LEIS, theory and experiment are in excellent agreement. It would be interesting to de-

termine the diffusion barrier of vacancies in this case and see how it compares to adatom diffusion. If our interpretation is correct, vacancies on Ag(100) should not be more mobile than adatoms on the same surface.

Finally, in view of the relatively small size of terraces in this last experiment, 8.5 atomic spacings, it is not clear that this geometry can effectively be used to determine diffusion barriers appropriate to infinitely wide terraces: In the case of Ir/Ir(111), for instance, it was noted (using FIM) that no adatoms are ever found in a region of width 3 nearest-neighbor distances from steps,⁷⁷ likely the consequence of a lower diffusion barrier in the vicinity of steps. Such an effect could bias experimental estimates of the barriers in cases where the depletion zone is a large fraction of the diffusion length, possibly the case in the above LEIS measurements.

In the last two experiments of interest,^{24,25} the separation of islands was measured and related to energy barriers through rate equations, assuming adatoms are the only mobile species (i.e., all larger clusters remain immobile and unable to dissociate.) While the published results are different, 0.28 ± 0.06 eV (Ref. 24) and 0.36 ± 0.03 eV (Ref. 25), the data of Ref. 24 was recently reinterpreted,⁷⁸ leading to a value of about 0.40 eV, in line with other experiments.

Grosso modo, from the above experiments, the diffusion barrier can be taken as 0.40 ± 0.05 eV. This is reasonably close to our GGA value (for adatom jumps) of 0.52 ± 0.05 eV, but the deviation is large enough to warrant closer examination. There are evidently two possibilities. First, the theoretical value may be in error, either because of model limitations (e.g., size), or because of a poor description of the exchange-correlation energy. We have at present no way of assessing these further. Second, it is possible that the assumptions underlying the interpretation of experimental data may not be fully justified. We have mentioned already that vacancies or limited terrace size could possibly play a role in the interpretation of LEIS measurements. In what follows, we examine more closely the assumptions behind rate equations.

In a rate-equation analysis, the diffusion coefficient depends on the island separation through a power law. If only adatoms are mobile, the exponent is 6. In a plot of the logarithm of island separation versus inverse temperature, the slope is simply the diffusion barrier for adatoms divided by this exponent. If dimers (and only dimers) can dissociate, then the exponent is 4 and the slope is now related not only to the adatom barrier but to the sum of adatom barrier and binding energy per atom of the dimer. Thus, clearly, detailed knowledge of the surface kinetics, as well as highly accurate data, are essential for extracting meaningful numbers from such measurements. Our calculations indicate that the diffusion barriers for adatoms and dimers are very close to one another and suggest, therefore, that the assumptions underlying the rate-equation analysis might not be valid.

A first assumption concerns the stability, against dif-

fusion and dissociation, of small clusters, which determines the exact form of the island-separation–diffusion-coefficient scaling relation. Experiment suggests that, at low flux and low enough temperatures — below 223 K — only adatoms are mobile.¹⁵ Above 223 K, dimers and trimers can dissociate, and thus change the scaling relation. According to our results, however, as discussed in Sec. III B 2, dimers should be mobile before they can dissociate. At 223 K, indeed, we find the rate of jump for dimers (i.e., non dissociated) to be approximately 10% that for adatoms (assuming similar prefactors). This, of course, affects the scaling relation and, therefore, the value of the barrier that can be inferred from the experimental data. In a recent Monte Carlo study of nucleation on Pt(111),⁷⁹ it was found that the island density remains unaltered in presence of dimer diffusion, as long as the barrier for the latter is *at least* 0.09 eV higher than the barrier for adatom diffusion. The difference between the two barriers here is 0.05 eV, thus suggesting that dimer mobility *cannot* be neglected.

Interestingly, the island separation at this same temperature, 223 K, can be reproduced by Monte Carlo simulations assuming that islands are square and that adatoms only are mobile.¹⁶ The jump frequency required to obtain satisfactory agreement with experiment is found to be 450 s^{-1} . Assuming a prefactor of 20 THz, as obtained in the present work, this translates into an energy barrier of 0.47 eV, now within the error bar of our theoretical prediction. This is strong indication that an imperfect scaling relation in the rate equations can lead to significant errors in experimental diffusion barriers.

When temperature is higher than 223 K, dimers are found to dissociate. Using rate equations, and assuming the smallest stable (“critical”) island to be the tetramer, Dürr and coworkers²⁵ estimated a binding energy of 0.08 eV for the dimer. This is much less than the value we find — 0.35 eV from EAM and 0.22 eV from first principles (cf. Table III). However, these data were recently reinterpreted by Bartelt and coworkers.⁵ They found that the change of the scaling relation occurring at 223 K is due to a gradual transition in critical island size, related to the onset of dimer dissociation, and not to a sharp transition from the adatom to the tetramer as assumed in Ref. 25. In this way, a dimer binding energy of 0.20–0.23 eV is obtained, in excellent agreement with the present calculations. It should be said, however, that the latter value was obtained assuming an energy barrier of 0.40 eV for the adatom, rather than 0.52 eV from the present theory.

To conclude on this point, it appears that dimer mobility has to be taken into account in order to describe correctly low-temperature growth on Cu(100). (We have not explored, because of computer limitations, the possibility that trimers also contribute, but this should not be completely ruled out.) This results in a very complicated scaling relation and therefore potentially significant errors in estimates of the energy barriers for diffusion.

We now discuss the shape of islands. We have found, from our MD/EAM simulations, that the barrier for dif-

fusion along steps is much smaller than that for diffusion on flat (100) surfaces — 0.26 vs 0.50 eV. (We expect, in view of the agreement for other barriers, that *ab initio* calculations would lead to equivalent results.) Thus we predict that the shape of islands will remain close to equilibrium, i.e., square, during growth as indeed is observed experimentally.²⁵ There exists, to our knowledge, only two experimental reports of this barrier, and they disagree sharply: In Ref. 80, a barrier of approximately 0.1 eV is given, consistent with the observed island shape. The other, Ref. 81, in contrast, reports a very high value of 0.45 eV, comparable to the barrier for diffusion on (100) terraces, and very likely too high to yield the correct island shape. Clearly, more measurements are needed to resolve this point.

V. CONCLUDING REMARKS

We have presented a detailed study of the diffusion of adatoms, dimers, and vacancies on Cu(100), using both *ab initio* static relaxation methods and semi-empirical simulations. Our results are discussed in the context of recent submonolayer growth experiments. We find that the GGA offers a much better description of the energetics of diffusion than the LDA, while the EAM yields generally satisfactory results, in addition to providing information on attempt-to-diffuse frequencies (prefactors). Vacancy diffusion is found to be the most favorable mechanism for mass transport, but is not necessary dominant, as it depends on details of the experiments. The value we obtain for the energy barrier for adatom diffusion is slightly larger than the available experimental numbers. However, we have demonstrated that the complexity of the scaling relations obtained from rate equations (and used to interpret the experimental measurements), arising for instance from small cluster mobility, could easily explain this discrepancy: Indeed, we have found that, at low temperatures, dimers are mobile, though to a lesser extent than adatoms. Dimers are also found to diffuse more readily than they dissociate. The preferred diffusion mechanism is the jump, for both the adatom and the dimer, i.e., exchange processes do not seem to be an important route for diffusion on this surface at low temperatures. Finally, our MD study of diffusion of adatoms, vacancies, and dimers revealed no clear dependence of the prefactors on the diffusing species and, in all cases, the static barrier was found to approximate well the dynamical barrier. From the present study, we conclude that a combination of highly-accurate *ab initio* static calculations and semi-empirical MD simulations provides a good basis for determining diffusion processes relevant to growth.

ACKNOWLEDGMENTS

We are grateful to Martin Fuchs for help with the pseudopotential generation and to Normand Mousseau, Risto Nieminen, Christian Ratsch, Ari Seitsonen, Matthias Scheffler, and Byung Deok Yu for stimulating discussions. This work was supported by grants from the Natural Sciences and Engineering Research Council (NSERC) of Canada and the “Fonds pour la formation de chercheurs et l’aide à la recherche” (FCAR) of the Province of Québec. One of us (G.B.) is thankful to NSERC and FCAR for financial support. We are grateful to the “Services informatiques de l’Université de Montréal” for generous allocations of computer resources. Part of the work reported here has been performed on the IBM/SP-2 from CACBUS (“Centre d’applications du calcul parallèle de l’Université de Sherbrooke”).

* e-mail: boisver@physcn.umontreal.ca

† To whom correspondence should be addressed; e-mail: lewis@physcn.umontreal.ca

¹ T. Ala-Nissila and S.C. Ying, Prog. Surf. Sci. **39**, 227 (1992).

² For a recent review of diffusion coefficient obtained through FIM, see G.L. Kellogg, Surf. Sci. Reports **21**, 1 (1994).

³ J. A. Venables, Philos. Mag. **27**, 697 (1973).

⁴ C. Ratsch, P. Šmilauer, A. Zangwill, and D.D. Vvedensky, Surf. Sci. **329**, L599 (1995).

⁵ M.C. Bartelt, L.S. Perkins, and J.W. Evans, Surf. Sci. Lett. **344**, L1193 (1995).

⁶ G. Boisvert, L.J. Lewis, and A. Yelon, Phys. Rev. Lett. **75**, 469 (1995).

⁷ P. Hohenberg and W. Kohn, Phys. Rev. **136**, B864 (1964); W. Kohn and L.J. Sham, Phys. Rev. **140**, A1133 (1965).

⁸ M. Methfessel, Phys. Rev. B **38**, 1537 (1988); M. Methfessel, C.O. Rodriguez, and O.K. Andersen, Phys. Rev. B **40**, 2009 (1989).

⁹ See, e.g., M.C. Payne, M.P. Teter, D.C. Allan, T.A. Arias, and J.D. Joannopoulos, Rev. Mod. Phys. **64**, 1045 (1992).

¹⁰ A. Khein, D.J. Singh, and C.J. Umrigar, Phys. Rev. B **51**, 4105 (1995).

¹¹ P.H. Philipsen and E.J. Baerends, Phys. Rev. B **54**, 5326 (1996).

¹² C. Lee, G.T. Barkema, M. Breeman, A. Pasquarello, and R. Car, Surf. Sci. Lett. **306**, L575 (1994).

¹³ H.-J. Ernst, F. Fabre, and J. Lapujoulade, Surf. Sci. Lett. **275**, L682 (1992).

¹⁴ H.-J. Ernst, F. Fabre, R. Folkerts, and J. Lapujoulade, Phys. Rev. Lett. **72**, 112 (1994).

¹⁵ J.-K. Zuo, J.F. Wendelken, H. Dürr, and C.-L. Liu, Phys. Rev. Lett. **72**, 3064 (1994).

¹⁶ M.C. Bartelt and J.W. Evans, Surf. Sci. **298**, 421 (1993).

¹⁷ M. Breeman, G.T. Barkema, and D.O. Boerma, Surf. Sci. **307-309**, 526 (1994).

- ¹⁸ G.T. Barkema, O. Biham, M. Breeman, D.O. Boerma, and G. Vidali, Surf. Sci. Lett. **306**, L569 (1994).
- ¹⁹ O. Biham, G.T. Barkema, and M. Breeman, Surf. Sci. **324**, 47 (1995).
- ²⁰ M.C. Bartelt and J.W. Evans, Phys. Rev. Lett. **75**, 4250 (1995).
- ²¹ M.C. Bartelt, S. Günther, E. Kopatzki, R.J. Behm, and J.W. Evans, Phys. Rev. B **53**, 4099 (1996).
- ²² J.J. De Miguel, A. Sánchez, A. Cebollada, J.M. Gallego, J. Ferrón, and S. Ferrer, Surf. Sci. **189/190**, 1062 (1987).
- ²³ M. Breeman and D.O. Boerma, Surf. Sci. **269/270**, 224 (1992).
- ²⁴ H.-J. Ernst, F. Fabre, and J. Lapujoulade, Phys. Rev. B **46**, 1929 (1992).
- ²⁵ H. Dürr, J.F. Wendelken, and J.-K. Zuo, Surf. Sci. Lett. **328**, L527 (1995).
- ²⁶ C.L. Liu, J.M. Cohen, J.B. Adams, and A.F. Voter, Surf. Sci. **253**, 334 (1991).
- ²⁷ L. Hansen, P. Stoltze, K.W. Jacobsen, and J.K. Nørskov, Phys. Rev. B **44**, 6523 (1991).
- ²⁸ D.E. Sanders and A.E. DePristo, Surf. Sci. **260**, 116 (1992).
- ²⁹ L.B. Hansen, P. Stoltze, K.W. Jacobsen, and J.K. Nørskov, Surf. Sci. **289**, 68 (1993).
- ³⁰ M. Breeman and D.O. Boerma, Surf. Sci. **287/288**, 881 (1993).
- ³¹ L.S. Perkins and A.E. DePristo, Surf. Sci. **294**, 67 (1993).
- ³² J.E. Black and Z.-J. Tian, Phys. Rev. Lett. **71**, 2445 (1993).
- ³³ C.L. Liu, Surf. Sci. **316**, 294 (1994).
- ³⁴ P. Stoltze, J. Phys. Condens. Matter **6**, 9495 (1994).
- ³⁵ L.S. Perkins and A.E. DePristo, Surf. Sci. **325**, 169 (1995).
- ³⁶ M. Karimi, T. Tomkowski, G. Vidali, and O. Biham, Phys. Rev. B **52**, 5364 (1995).
- ³⁷ J. Merikoski and T. Ala-Nissila, Phys. Rev. B **52**, 8715 (1995).
- ³⁸ G.A. Evangelakis and N.I. Papanicolaou, Surf. Sci. **347**, 376 (1996).
- ³⁹ Z.-P. Shi, Z. Zhang, A.K. Swan, and J.F. Wendelken, Phys. Rev. Lett. **76**, 4927 (1996).
- ⁴⁰ P.V. Kumar, J.S. Raut, S.J. Warakowski, and K.A. Fichtorn, J. Chem. Phys. **105**, 686 (1996).
- ⁴¹ S.M. Foiles, M.I. Baskes, and M.S. Daw, Phys. Rev. B **33**, 7983 (1986).
- ⁴² J.B. Adams, S.M. Foiles, and W.G. Wolfer, J. Mater. Res. **4**, 102 (1989).
- ⁴³ S.M. Foiles in *Equilibrium Structure and Properties of Surfaces and Interfaces*, ed. by A. Gonis and G.M. Stocks (Plenum, New York, 1992) p.89.
- ⁴⁴ G. Boisvert and L.J. Lewis, Phys. Rev. B **54**, 2880 (1996).
- ⁴⁵ G. Boisvert, L.J. Lewis, M.J. Puska, and R.M. Nieminen, Phys. Rev. B **52**, 9078 (1995).
- ⁴⁶ D.M. Ceperley and B.J. Alder, Phys. Rev. Lett. **45**, 566 (1980); J. Perdew and A. Zunger, Phys. Rev. B **23**, 5048 (1981).
- ⁴⁷ N. Troullier and J.L. Martins, Solid State Commun. **74**, 613 (1990); Phys. Rev. B **43**, 1993 (1991).
- ⁴⁸ L. Kleinman and D.M. Bylander, Phys. Rev. Lett. **48**, 1425 (1982).
- ⁴⁹ X. Gonze, R. Stumpf, and M. Scheffler, Phys. Rev. B **44**, 8503 (1991).
- ⁵⁰ M. Fuchs *et al.*, in preparation.
- ⁵¹ J.P. Perdew, J.A. Chevary, S.H. Vosko, K.A. Jackson, M.R. Pederson, D.J. Singh, and C. Fiolhais, Phys. Rev. B **46**, 6671 (1992).
- ⁵² A. Kley *et al.*, in preparation.
- ⁵³ R. Car and M. Parrinello, Phys. Rev. Lett. **55**, 2471 (1985).
- ⁵⁴ R. Stumpf and M. Scheffler, Computer Phys. Commun. **79**, 447 (1994).
- ⁵⁵ T. Korhonen, M.J. Puska, and R.M. Nieminen, Phys. Rev. B **51**, 9526 (1995).
- ⁵⁶ H.M. Polatoglou, M. Methfessel, and M. Scheffler, Phys. Rev. B **48**, 1877 (1993).
- ⁵⁷ Z.W. Lu, S.-H. Wei, and A. Zunger, Phys. Rev. B **41**, 2699 (1990).
- ⁵⁸ T. Kraft, P.M. Marcus, M. Methfessel, and M. Scheffler, Phys. Rev. B **48**, 5886 (1993).
- ⁵⁹ Th. Rodach, K.-P. Bohnen, and K.M. Ho, Surf. Sci. **286**, 66 (1993).
- ⁶⁰ M.H. Kang, R.C. Tartar, E.J. Mele, and P. Soven, Phys. Rev. B **35**, 5457 (1987).
- ⁶¹ J.R. Chelikowski and M.Y. Chou, Phys. Rev. B **38**, 7966 (1988).
- ⁶² S. Jeong, Phys. Rev. B **53**, 13 973 (1996).
- ⁶³ Y.S. Touloukian, R.K. Kirby, R.E. Taylor, and P.D. Desai, *Thermophysical Properties of Matter*, (IFI/Plenum, New York, 1977), Vol. 12.
- ⁶⁴ R. Richter, J.R. Smith, and J.G. Gray, in *The Structure of Surfaces I*, edited by M.A. van Hove and S.Y. Tong, Springer Series in Surface Science, Vol. 2 (Springer, Berlin, 1985), p.38.
- ⁶⁵ D.M. Lind, F.B. Dunning, G.K. Walters, and H.L. Davis, Phys. Rev. B **35**, 9037 (1987).
- ⁶⁶ P.O. Gartland, S. Berge, and B.J. Slagsvold, Phys. Rev. Lett. **28**, 738 (1972).
- ⁶⁷ G.A. Haas and R.E. Thomas, J. Appl. Phys. **48**, 86 (1977).
- ⁶⁸ L. Peralta, E. Margot, Y. Berthier, and J. Oudar, J. Microsc. Spectrosc. Electron **3**, 151 (1978).
- ⁶⁹ G. Boisvert and L.J. Lewis, unpublished.
- ⁷⁰ G. Boisvert, L.J. Lewis, and M. Scheffler, manuscript in preparation.
- ⁷¹ B.D. Yu and M. Scheffler, Phys. Rev. Lett. **77**, 1095 (1996).
- ⁷² The value of 0.35 eV is not converged with respect to size; using a larger model, an energy of 0.43 eV is obtained (M. Karimi, private communication).
- ⁷³ M.H. Langelaar, M. Breeman, and D.O. Boerma, Surf. Sci. **352-354**, 597 (1996).
- ⁷⁴ T.J. Raeker, L.S. Perkins, and L. Yang, Phys. Rev. B **54**, 5908 (1996).
- ⁷⁵ J.C. Tully, G.H. Gilmer, and M. Shugard, J. Chem. Phys. **71**, 1630 (1979).
- ⁷⁶ M. Breeman, G.T. Barkema, and D.O. Boerma, Surf. Sci. **303**, 25 (1994).
- ⁷⁷ S.C. Wang and G. Ehrlich, Phys. Rev. Lett. **70**, 41 (1993).
- ⁷⁸ H.J. Ernst, private communication.
- ⁷⁹ M. Bott, M. Hohage, M. Morgenstern, T. Michely, and G. Comsa, Phys. Rev. Lett. **76**, 1304 (1996).
- ⁸⁰ M. Poensgen, J.F. Wolf, J. Frohn, M. Giesen, and H. Ibach, Surf. Sci. **274**, 430 (1992).
- ⁸¹ J.C. Girard, S. Gauthier, S. Rousset, W. Sacks, S. de Cheveigné, and J. Klein, Surf. Sci. **301**, 245 (1994).

TABLE I. *Ab-initio* results for bulk Cu and the clean (100) surface; FP-LMTO and PP-PW refer to the all-electron and pseudopotential calculations from the present work. AE is for other all-electron calculations and PP for other pseudopotential calculations. LDA and GGA specify the level of approximation used for the exchange-correlation energy.

	Lattice constant	Surface energy	Surface relaxation		Work function
	a (Å)	σ (J/m ²)	Δd_{12} (% d_{bulk})	Δd_{23} (% d_{bulk})	W (eV)
FP-LMTO-LDA	3.50	1.85	-3.0	-	4.87
PP-PW-LDA	3.57	1.91	-3.5	0.0	4.86
PP-PW-GGA	3.68	1.42	-4.5	-0.4	4.42
AE-LDA	3.52 ^{10,55} , 3.55 ⁵⁶ , 3.56 ⁵⁷ , 3.58 ⁵⁸ , 3.61 ⁵⁷	-	-	-	-
AE-GGA	3.62 ¹⁰	-	-	-	-
PP-LDA	3.62 ⁵⁹⁻⁶¹ , 3.61 ⁶²	1.71 ⁵⁹	-3.02 ⁵⁹	0.08 ⁵⁹	4.95 ⁵⁹
expt.	3.60 ⁶³	2.02 ⁶⁴	-1.2 ⁶⁵	0.9 ⁶⁵	4.59 ⁶⁶ , 4.83 ⁶⁷ , 4.45 ⁶⁸

TABLE II. Diffusion barriers and prefactors for diffusion on Cu(100). The *ab initio* values are obtained using the GGA with a 4-layer, (3 × 3) cell. J and X are for jumps and exchanges, respectively. E_A^0 is the zero-temperature (static) value of the energy barrier while E_A and Γ_0 are determined from an Arrhenius fit to the MD data.

	EAM			<i>ab initio</i>
	Γ_0 (THz)	E_A (eV)	E_A^0 (eV)	E_A^0 (eV)
Adatom-J	20(e ^{±0.2})	0.49 ± 0.01	0.50	0.52 ± 0.05
Adatom-X	437(e ^{±0.7})	0.70 ± 0.04	0.73	0.96 ± 0.10
Dimer-J	13(e ^{±0.5})	0.48 ± 0.03	0.49	0.57 ± 0.06
Dimer-X	320(e ^{±0.8})	0.73 ± 0.05	0.74	0.79 ± 0.15
Vacancy	27(e ^{±0.7})	0.47 ± 0.05	0.47	0.42 ± 0.08
Along step	3.0(e ^{±0.2})	0.24 ± 0.02	0.26	-

TABLE III. Static properties of the dimer. The *ab initio* values are obtained using the GGA with a 4-layer, (3 × 3) cell. See the text for a definition of the exact and approximate forms of the dissociation energy.

	EAM (eV)	<i>ab initio</i> (eV)
Binding energy	0.35	0.22 ± 0.03
Dissociation energy (exact)	0.81	-
Dissociation energy (approx.)	0.85	0.74 ± 0.07
Metastable vs equilibrium	0.29	0.35 ± 0.04

TABLE IV. Diffusion barrier for the adatom (in eV) from first principles, as discussed in the text. The superscript “u” is for an unrelaxed substrate while “2” refers to the case where the top two layers of the substrate were relaxed; in all others, only the top layer relaxed only. “BZ” refers to a denser \mathbf{k} -point grid for Brillouin zone integration.

System	FP-LMTO LDA	PP-PW			
		LDA	GGA		
	jump	jump	exchange	jump	exchange
(2 x 2) cell:					
3 layers	-	0.75 ^u , 0.74	1.23 ^u , 1.18	-	-
4 layers	-	0.66, 0.65 ² , 0.68 ^{BZ}	1.05, 1.04 ² , 1.08 ^{BZ}	0.51	0.85
5 layers	0.69 ^u	0.69	1.04	0.55	0.82
6 layers	-	0.65	1.18	-	-
7 layers	0.66 ^u	0.69	1.13	-	-
9 layers	0.68 ^u	-	-	-	-
(3 x 3) cell:					
3 layers	-	0.75	1.03	-	-
4 layers	-	-	-	0.52	0.96
5 layers	0.65 ^u	-	-	-	-

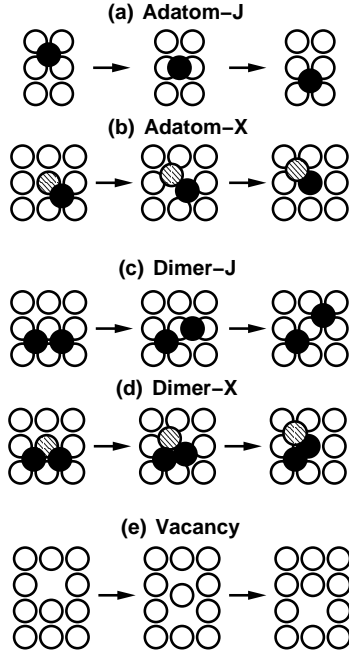
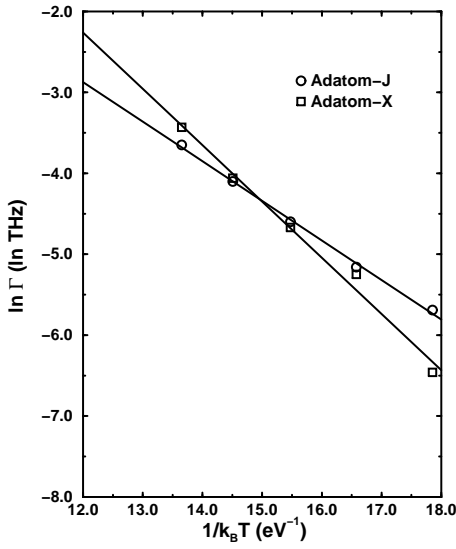
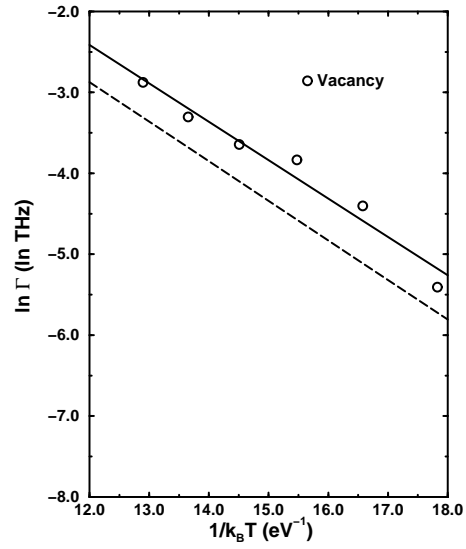


FIG. 1. The various diffusion processes studied in the present work; J and X refer to jump and exchange, respectively.
Boisvert and Lewis, Fig. 1



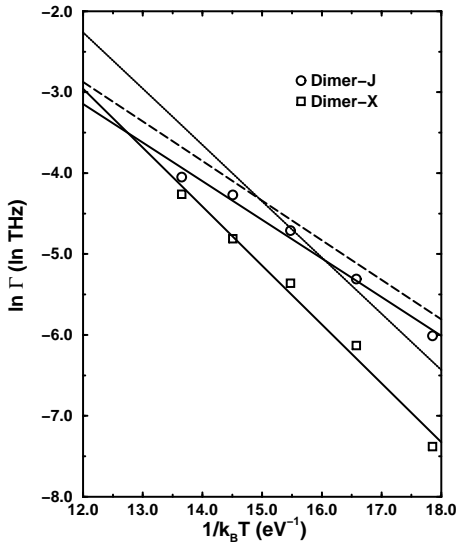
Boisvert and Lewis, Fig. 2

FIG. 2. Arrhenius plot of the frequency of jumps (J) and exchanges (X) for a Cu adatom on Cu(100). The solid lines are fits to the MD data.



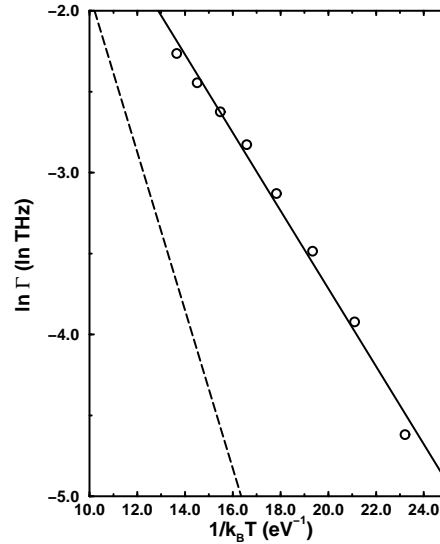
Boisvert and Lewis, Fig. 4

FIG. 4. Arrhenius plot of the frequency of jumps for vacancy diffusion on Cu(100). The solid line is a fit to the MD data. The dashed line is the corresponding frequency for adatom jumps.



Boisvert and Lewis, Fig. 3

FIG. 3. Arrhenius plot of the frequency of jumps (J) and exchanges (X) for a Cu dimer on Cu(100). The solid lines are fits to the MD data. The dashed and dotted line correspond to adatom jumps and exchanges, respectively.



Boisvert and Lewis, Fig. 5

FIG. 5. Arrhenius plot of the frequency of events for diffusion of a Cu atom along a step on Cu(100). The solid line is a fit to the MD data. The dashed line is the frequency of the corresponding mechanism on the clean surface.